Composite Material Hollow Core Fibers – functionalisation with silicon and 2D materials

A. Lewis, F. De Lucia, W. Belardi, F. Poletti, C. C. Huang, D. Hewak and P. J. A. Sazio*
Optoelectronics Research Centre, University of Southampton, SO17 1BJ, UK
*pjas@soton.ac.uk

ABSTRACT

Hollow Core Anti-resonant fibers allow for guidance of mid-infrared light at low attenuation and can be used for a variety of applications, such as high power laser transmission and gas sensing. Recent work has seen the integration of silicon[1] into such fibers with linear losses potentially as low as 0.1dB/m. Due to the change in refractive index difference of silicon via for example the free carrier plasma dispersion effect, the prospect of an all optical modulator using such a fiber has been proposed[1]. Here, further work has been undertaken on the integration of functional materials inside hollow core fibers via the deposition of the TMD semiconductor material MoS_2, in its few-layered form. Through the use of a liquid precursor, a high quality MoS_2 film can be deposited over 30cm length of fiber, as confirmed via Raman spectroscopy. The transmission spectra of these novel composite material hollow core fibers has also been analysed, showing additional loss of around 5dB/m, despite being only around 2nm in thickness. This implies that the refractive index of the integrated material is potentially able to modify the guidance properties of the fiber sample. We will present a comparison of the composite material hollow core fibers we have fabricated to date and discuss the prospects for using these novel waveguides in the active manipulation of light, including optical switching, sensing and frequency generation.

1. INTRODUCTION

Hollow core waveguides such as the antiresonant fibers[1] (ARFs) shown in Figure 1, can allow for high power guidance and low optical loss in wavelength regions where standard step index based glass fiber waveguides will absorb light very strongly. The highly extended light-matter interaction afforded by hollow core fiber designs has seen growth in gas[2] sensor applications as well as mid-IR light generation in gas-filled structures[3].

In planar geometries, recent research has focused on the use of transition metal dichalcogenides (TMDCs) in optical devices. These materials can be utilised in a monolayer form[4], much like graphene and a wide variety of different TMDC deposition and exfoliation methods have been explored. In comparison to bulk semiconductors,

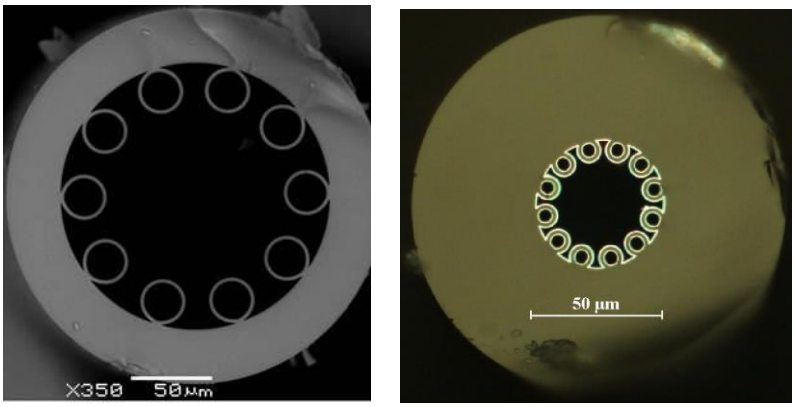

Figure 1. RHS Hollow antiresonant fibre(ARF) with detached cladding tubes[3]. LHS Composite material hollow antiresonant fibre: the white lines show a:Si-H deposited on the internal and external cladding tube of a borosilicate based hollow fibre[1].

thin TMDC layers have relatively small overall optical absorption due to their low dimensional nature, whilst exhibiting many useful optical properties, such as high nonlinearity and a large electronic bandgap. Exploitation of these properties within waveguides will lead to a raft of applications for the technology.

There is a rich history of silicon based optical fibers[5]. In most cases, this refers to the deposition of silicon in the core of a hollow core fiber, thus creating a step-index fiber. However, this technology is limited by large losses, despite all-optical modulators having being demonstrated to date[6]. Previous works on combining 2D TMDC materials and fibers are somewhat different. The combination of the two technologies has seen prevalence in the sensor market and the use of TMDCs as saturable absorbers. The use of D-shaped[7] or tapered fibers[8] are common, with the TMDC deposited on the surface of the fiber. Exfoliation from bulk natural crystalline TMDC materials, as well as CVD deposition techniques are typically used to transfer the layers onto the fiber surfaces.

Recent work from our group has seen the integration of silicon into hollow core negative fiber structures, as detailed by Belardi *et al*[1]. Theoretical simulations of such composite material ARFs (CM-ARFs), indicate potential low loss operation of around 0.1dB/m. Further work showed evidence that such fiber structures still maintained guidance via the antiresonant condition. The fiber was realised experimentally via the decomposition of Silane gas at high temperature, which would leave behind a layer of silicon on the inside of the fiber[1]. However, the precursor gas has safety issues regarding the fact it is extremely pyrophoric.

The ever increasing research done on TMDC materials offer an intriguing alternative. For example, Du *et al.* placed exfoliated MoS_2 flakes onto the core of a standard step index optical fiber, which had been exposed via etching[9]. The power guided down the fiber was modulated by the humidity of the surrounding area, with a quick response time. MoS_2 and WS_2 have also been seen to be good saturable absorbers in fiber lasers in passive mode-locking and Q-switching regimes[7,10]. Usually these are fabricated by TMDC layer transfer onto the fiber.

However, there are instances whereby the active 2D film is deposited straight onto the functionalised area of the fiber. This can be seen in work by Li *et al.* whereby the precursor ammonium tetrathiomolybdate was decomposed onto the surface of a U-bent tapered fiber[8]. This created a conformal MoS_2 film on the fiber, which was able to sense the presence of ethanol. The created film was found to be bilayer.

We therefore turn our attention to the functionalisation of hollow core optical fibers with these 2D films. Based on previous work from within our group, we aim to use the same negative curvature hollow fiber structures to create an optical device.

Recently it has been observed that TMDC materials are able to demonstrate electro-optical effects, affecting both the materials' absorption and refractive index. This is highlighted in Yu *et al.*'s work, showing a dramatic change in the refractive index[11] of WS_2. Once gated, the real part of the refractive index changed from 4.80 to 3.97. The authors also note MoS_2's capability in this regard. It is therefore possible to envisage a device that uses this ability to modulate incoming signals.

The basis of this work revolves around the numerical simulations performed on these fiber structures. We begin by showing these results in the next section, followed by some preliminary experimental work we have carried

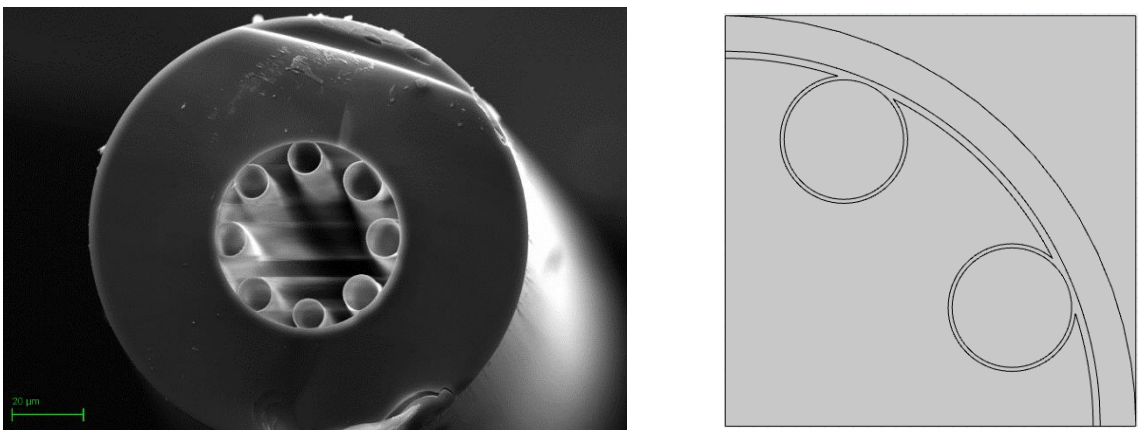

Figure 2. RHS shows an SEM image of the modelled and experimentally realised hollow core ARF fiber. LHS shows the structure of the hollow core fiber being simulated.

out. This is followed by the discussion of these results. We finally address our conclusions of the current work, and suggest future improvements.

2. SIMULATIONS RESULTS

To begin the simulations, the initial fiber structures were created in COMSOL Multiphysics as seen in Figure 2b. This was modelled as an 8 ring negative curvature fiber structure, made of borosilicate glass, with a (constant) refractive index of 1.473. The characteristics of the fiber were as follows: a core size of 16.88um, the cladding ring radius of 4.475um with a glass thickness of 282.9nm, as confirmed by the SEM image in figure 2a. Numerical simulations of this glass/air fiber resulted in the 'empty' trace seen in Figure 3.

This was followed by adding the composite material into the fiber simulation. To create a MoS_2 film, the thickness of the material was chosen at a range of different values. This ranged from 10nm, which could be considered as 'bulk' material, to 5nm that would correspond to around 6 layered material, to 3nm, which we could class as a three layered film. The refractive index of the material was based on work from Liu *et al.* and was selected as 4.2936[12]. It is at around this value whereby the refractive index of MoS_2 begins to become constant as a function of wavelength. It is also in this wavelength region where the majority of the simulations efforts were performed.

As seen from figures 4a and 4b, with the addition of the composite film a second resonance appears. The position of this peak is dependent on the thickness of the additional film, whereas the original peak does not seem to alter its position. Upon further testing, the location of these peaks appeared dependent only on the refractive index and the thickness of the film. This was confirmed by replacing the film with WS_2. The refractive index was changed to 4.80, as discussed[11] by Yu *et al.* A second model was created with the refractive index changed to 3.97, as if the film had been electrically gated. As seen, a significant rise in the leakage loss occurs, with a blue shift when the refractive index is higher. Our next aim to produce this technology in experimental form. The simulations results are shown in figure 5.

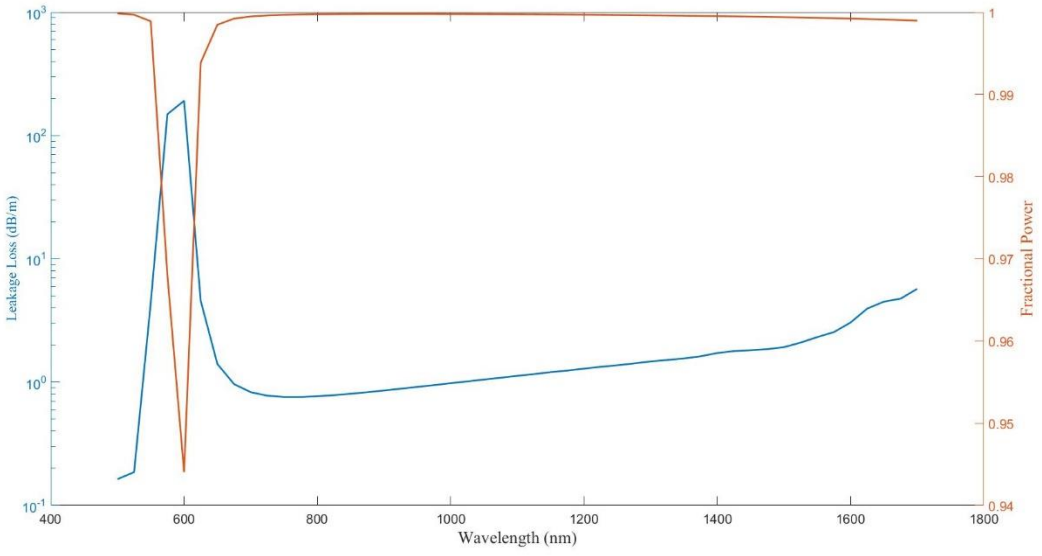

Figure 3. Numerical simulations demonstrate the loss of the fiber shown in Figure 2b when the fiber has no deposition inside. As can be seen, a single resonance occurs at around the 600nm mark. The Y axis labels show leakage loss (LHS) and the fraction of power residing in the fiber core (RHS)

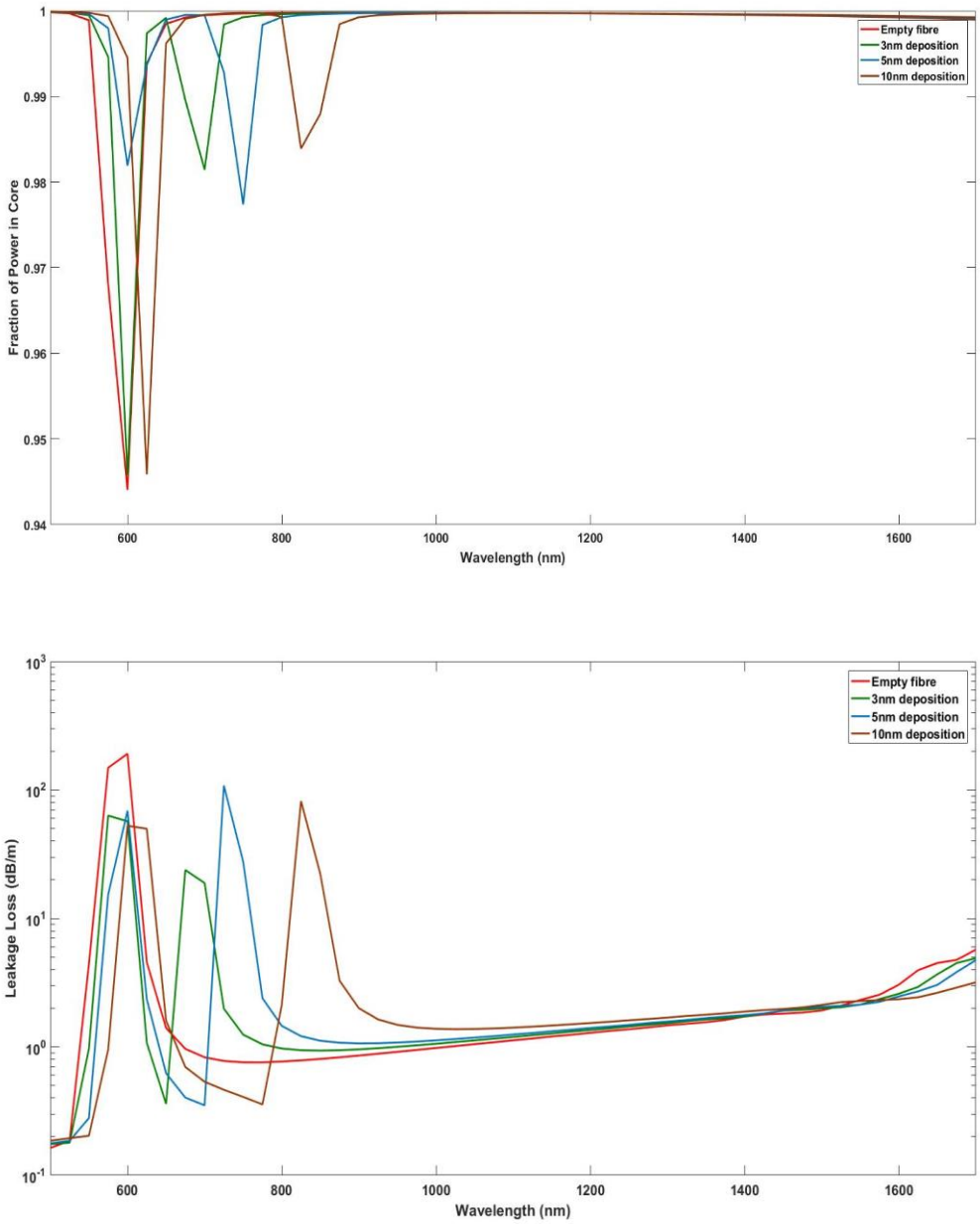

Figure 4a. Numerical simulation results of the MoS_2 deposition for an increasing thickness of film. It is computationally limited at 3nm. The first graph shows the confinement in the core of the fiber. Figure 4b shows the result of the fiber with increasing film thickness and calculates the leakage loss of the fiber.

3. EXPERIMENTAL RESULTS

Following the numerical simulation effort, the fabricated borosilicate fiber shown in Figure 2a was functionalised with TMDC layers using a liquid phase precursor to allow deposition inside the fiber, whilst leaving the outside of the fiber free from contamination. A 1wt% solution was created with the precursor ammonium tetrathiomolybdate mixed into a solvent solution of 4.5ml DMF, 4.5ml butylamine and 1ml of amino-ethanol following work from Yang. J *et al*[13]. The solution was allowed to flow through the fiber via capillary action. The fiber was then placed on the inside of a tube furnace to be annealed. The conditions of such were a $500^{O}C$ dwell for 2 hours, whilst in a hydrogen/argon atmosphere.

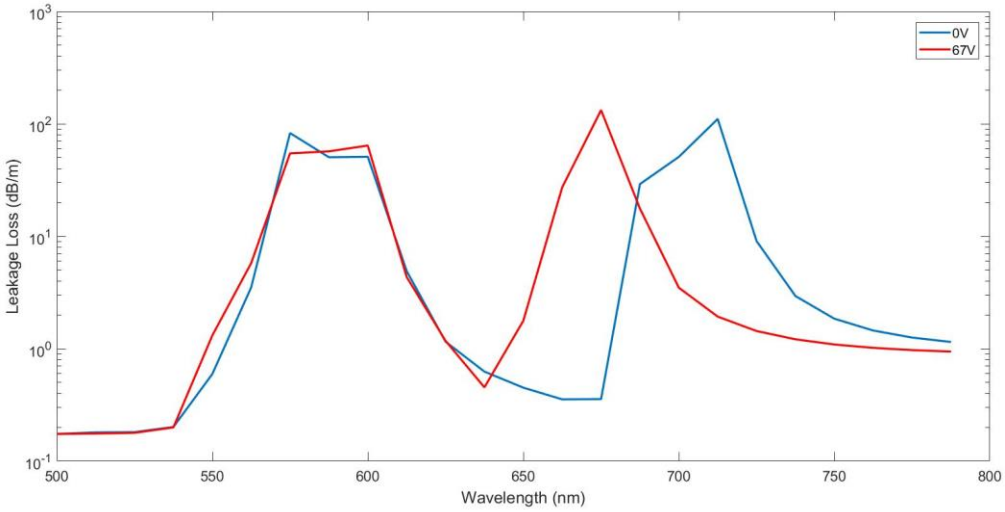

Figure 5 shows the simulated guidance properties of a WS_2 integrated hollow core fiber. There are two instances shown, one for a fiber with an external voltage of 0V, one for a fiber with an external voltage of 67V. The change in voltage changes the refractive index of the composite material ARF.

The resulting fiber was then analysed via Raman scattering as shown in Figure 6, which shows a trace confirming the presence of MoS_2 with peaks at 379cm^{-1} and 402.5cm^{-1}. Traces much like Figure 6 were reproducible along a 30cm length of the fibre. From the Raman peak analysis, it can be assumed that the film is of 2-3 layer thickness. The uniformity of the film is uncertain, as the collected Raman scattering must travel through the fiber to reach the MoS_2 film, as seen in the inset of Figure 6.

An optical linear loss cutback measurement was then performed on the composite material ARF (CM-ARF) fiber. For this, a short length of fiber, 1m, was used, with 30cm of film deposited within the hollow core. Looking laterally at the fiber, this deposited region appeared obvious due to a darkened region in the fiber. The fiber was then connected to a white light source via a bare fiber adaptor, and plugged into an OSA, with the resulting spectral response of the CM-ARF is shown in Figure 7.

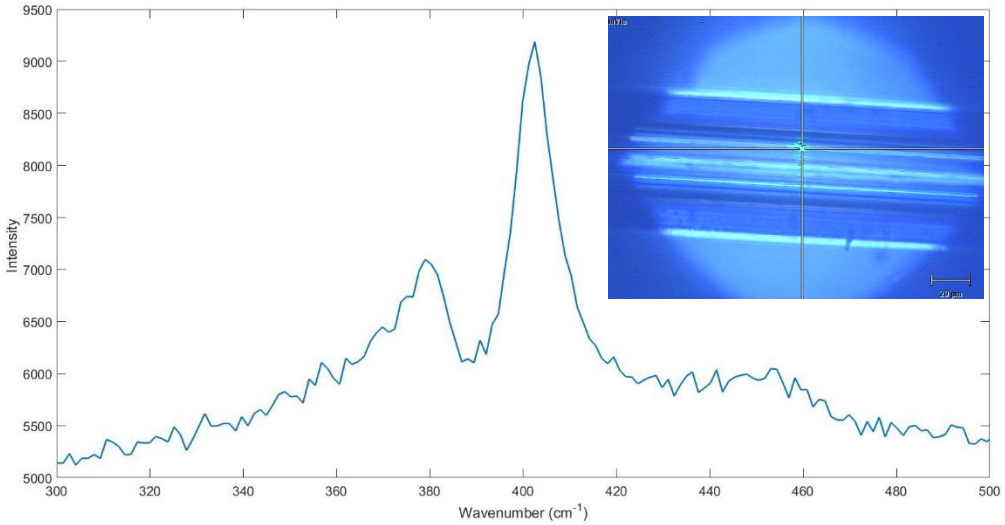

Figure 6 shows a Raman spectra obtained from the MoS_2 integrated CM-ARF. The peak positions are 379cm^{-1} and 402.5cm^{-1} wavenumbers, meaning a peak separation of 23.5cm^{-1}, corresponding to a trilayer film thickness. Inset is an image of the fiber under investigation, with the crosshairs showing where the Raman laser is being focussed.

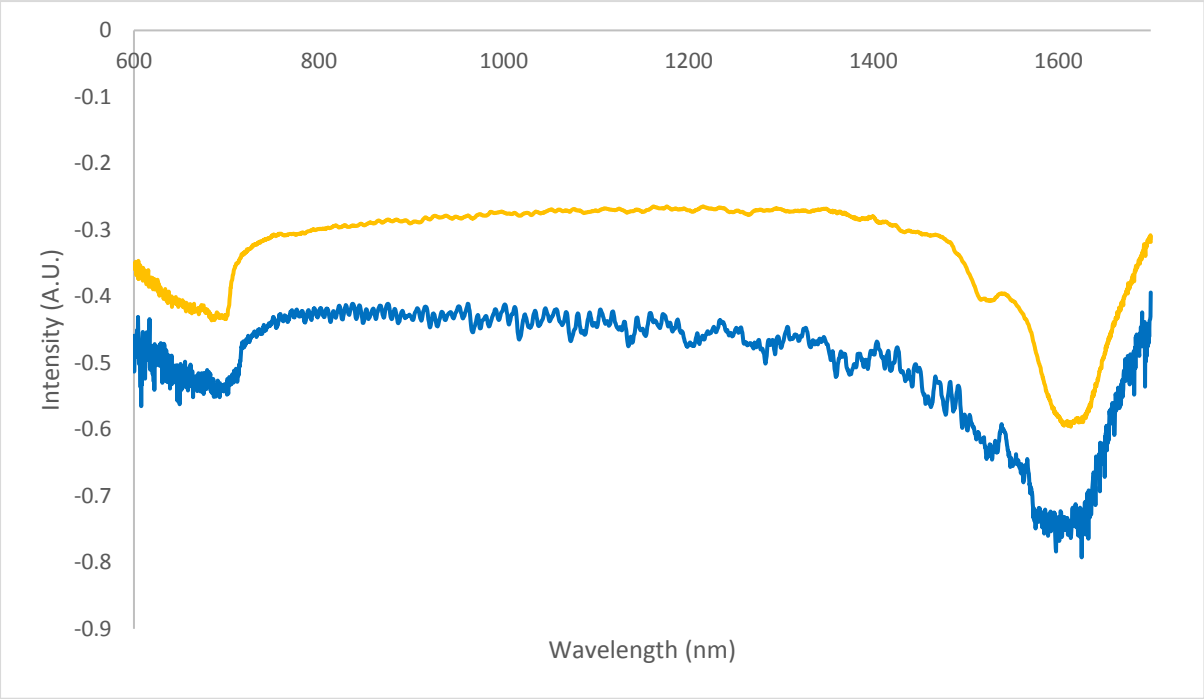

Figure 7 shows the traces of a molybdenum filled fiber of length 5m which is the blue trace. The yellow trace corresponds to that of the same fibre with the molybdenum sulphide region of length 30cm cleaved out, as well as 40cm of "empty" fiber. This is a fibre of length 4.3m.

4. DISCUSSION

When comparing the experimental and theoretical data, there is a significant difference. Our computational simulations suggest that the addition of a MoS_2 film should generate a second resonance to the loss of the fiber, as well as cause a small shift in the original resonance peak. However, this is not yet confirmed by our experimental work. This may be caused by micro fractures or uneven inner rings within the fiber, caused by handling or at the manufacturing stage. To test this, the experiment will be repeated in a new fiber. Furthermore, when looking into its possible synthesis routes, it appears that the same process being carried out on MoS_2 could be used to generate tungsten disulphide films which can have superior optical properties for future fiber devices.

5. CONCLUSION

Our theoretical findings appear to offer 2D TMDC films as excellent alternatives to bulk semiconductors such as silicon when deposited into the inner surfaces of a negative curvature optical fiber. When looking into the additional loss the insertion of such a film would create, our numerical models suggest that the potential loss of less than 1dB/m can occur at guidance wavelengths of 1550nm. They also show how an additional resonance band appears in the fiber transmission spectrum. However, this is yet not confirmed by our experimental work. This second band does not seem to appear, although a variation does occur in Figure 7, implying the integrated MoS_2 does indeed have an effect on the guided light. Reproducibility of such traces was difficult, suggesting the fiber type being experimented with was imperfect.

Further work looking into simulating a gating mechanism within a WS_2 film also appears feasible. Through use of the electro-optical effect, the change in the refractive index of the material is able to influence the position of the resonant peak. This could therefore suggest tungsten disulphide integrated fibers in modulation devices.

REFERENCES

[1] Belardi,. W. *et al*., "Composite material hollow antiresonant fibers", Optics Letters 42(13), 2535-2538 (2007).
[2] Jin, W. *et al.,* "Gas detection with micro- and nano-engineered optical fibers", Optical Fiber Technology 19(6), 741- 759 (2013).
[3] Wang, Z. *et al.*, "Efficient diode-pumped mid-infrared emission from acetylene-filled hollow-core fiber", Opt. Expr. 22(18), 21872-21878 (2014).
[4] Li, X. and Zhu, H., "Two-dimensional MoS2: Properties, preparation, and applications", Journal of Materiomics 1(1), 33-44 (2015).
[5] He R. *et al.*. "Silicon p-i-n Junction Fibers", Adv. Mater. 25, 1461–1467 (2013).
[6] Won, D.J. *et al.*, "All-optical modulation of laser light in amorphous silicon-filled microstructured optical fibers", Appl. Phys. Lett. 91(16), 161112 (2007).
[7] Aiub, E. J. *et al.* "200-fs mode-locked Erbium-doped fiber laser by using mechanically exfoliated MoS2 saturable absorber onto D-shaped optical fiber" Opt. Expr. 25 (9), 10546-10552 (2017).
[8] Li, Z. *et al*. "Evanescent wave absorption sensor with direct-growth MoS2 film based on U-bent tapered multimode fiber." J. Phys. D: Appl. Phys. 50, 315302 (2017).
[9] Du, B. *et al.* "MoS2-based all-fiber humidity sensor for monitoring human breath with fast response and recovery." Sensors and Actuators B 251, 180-184 (2017)
[10] Wu, K. *et al.* "WS2 as a saturable absorber for ultrafast photonic applications of mode-locked and Q-switched lasers" Opt. Expr. 23(9), 11453-11461 (2015).
[11] Yu, Y. *et al.* "Giant Gating Tunability of Optical Refractive Index in Transition Metal Dichalcogenide Monolayers" Nano Lett. 17 (6), 3613–3618 (2017).
[12] Liu, H.L. *et al.* "Optical properties of monolayer transition metal dichalcogenides probed by spectroscopic ellipsometry". Appl. Phys. Lett. 105, 201905 (2014)
[13] Yang, J. *et al.* "Wafer-scale synthesis of thickness-controllable MoS2 films via solution-processing using a dimethylformamide/n-butylamine/2-aminoethanol solvent system." Nanoscale 7, 9311-9319 (2015)